

000 001 002 003 004 005 006 007 008 009 010 011 012 013 014 015 016 017 018 019 020 021 022 023 024 025 026 027 028 029 030 031 032 033 034 035 036 037 038 039 040 041 042 043 044 045 046 047 048 049 050 051 052 053 FED MOBILLM: EFFICIENT FEDERATED LLM FINE-TUNING OVER HETEROGENEOUS MOBILE DEVICES VIA SERVER ASSISTED SIDE-TUNING

006
007 **Anonymous authors**
008 Paper under double-blind review

010 ABSTRACT

013 Collaboratively fine-tuning (FT) large language models (LLMs) over heterogeneous
014 mobile devices fosters immense potential applications of personalized intelligence.
015 However, such a vision faces critical system challenges. Conventional federated
016 LLM FT approaches place prohibitive computational and memory burdens on
017 mobile hardware, and their synchronous model aggregation protocols stall for
018 slower devices. In this paper, we propose Fed MobiLLM, a novel design to
019 facilitate efficient federated LLM FT across mobile devices with diverse com-
020 puting/communication speeds and local model architectures. In particular, Fed
021 MobiLLM implements a pioneering server-assisted federated side-tuning paradigm.
022 Briefly, mobile devices perform lightweight forward propagation computations on
023 local data using their frozen pre-scaled backbone LLMs, and then upload selected
024 intermediate activations. The server trains a shared side-network independently,
025 eliminating client-side backpropagation and enabling asynchronous updates. To
026 bridge model heterogeneity across different devices, we introduce an adaptive
027 layer-wise feature alignment method, which ensures consistent representations
028 for collaboratively tuning a shared side network. Extensive experimental results
029 demonstrate that Fed MobiLLM can maintain robust fine-tuning performance
030 while achieving extremely low on-device memory, with at least 95.2% reduction in
031 computation overhead, 93.2% reduction in communication costs and 5.1 \times faster
032 convergence compared to existing methods, validating its efficacy for practical
033 LLM adaptation over heterogeneous mobile devices.

034 1 INTRODUCTION

035 Fine-tuning large language models (LLMs) for domain-specific tasks unlocks significant potential for
036 novel applications, driving growing demand for personalized intelligence. Data required for such task
037 adaptation is naturally generated and stored across massive personal mobile devices like smartphones
038 and wearables. However, due to privacy constraints, this decentralized data cannot be combined for
039 centralized training. Federated learning (FL) (McMahan et al., 2017) offers a promising paradigm for
040 enabling collaborative, privacy-preserving LLM fine-tuning across mobile devices while keeping raw
041 user data localized. While foundational models like GPT (Brown et al., 2020), BERT (Devlin et al.,
042 2018), and LLaMA (Touvron et al., 2023) demonstrate broad capabilities (Ren et al., 2024; Ye, 2024;
043 Brown et al., 2020), practical federated fine-tuning of LLMs faces critical bottlenecks due to mobile
044 devices’ limited computational power, memory capacity, and network bandwidth.

045 To tackle these resource constraints, recent work explores federated LLM FT with parameter-efficient
046 fine-tuning (PEFT) methods like Adapters (Houlsby et al., 2019) or LoRA (Hu et al., 2022). These
047 approaches follow the standard FL loop (local training \rightarrow upload \rightarrow server aggregation \rightarrow model
048 distribution), but exchanging only lightweight trainable modules (eg. LoRA) instead of full model
049 weights. While reducing client-side computation (due to fewer trainable parameters), local training
050 still requires storing LLM weights, intermediate activations and optimizer states—often exceeding
051 the memory capacity of mobile devices. For example, tuning a 1.3B-parameter model with LoRA
052 typically requires over 14.5 GB of GPU memory, which exceeds the 4–12 GB available on most
053 mobile devices (Li et al., 2025). Furthermore, the inherently synchronous aggregation protocol forces
the server to wait for multiple updates, resulting in significant resource waste when dealing with

054 heterogeneous devices; stragglers with slower computation or communication dramatically prolong
 055 convergence time—an issue amplified by the sheer size of modern LLMs.
 056

057 In this paper, we propose Fed MobiLLM, a novel and efficient federated LLM fine-tuning framework
 058 built upon the server-assisted side-tuning principle inspired by PAE MobiLLM (Yang et al., 2025).
 059 Specifically, we decouple resource-intensive gradient computation from mobile devices by hosting
 060 all trainable parameters within a shared side-network on the server, while each mobile device
 061 retains only its frozen backbone LLM. During federated fine-tuning, each mobile device executes
 062 forward propagation computations on local data using its frozen backbone and uploads selected
 063 intermediate activations to the server. The server performs asynchronous backpropagation using
 064 these activations, computing gradients and updating the shared side-network independently for each
 065 mobile device’s activations - without requiring global synchronization. In this way, Fed MobiLLM
 066 allows mobile devices to bypass costly on-device backpropagation and optimizer steps, drastically
 067 reducing client memory and computational load. Crucially, by enabling server-side side-network
 068 training to proceed immediately upon receiving any mobile device’s activations, Fed MobiLLM
 069 eliminates the fundamental straggler bottleneck inherent in synchronous FL aggregation protocols.
 070 Fed MobiLLM thus offers a mobile device-friendly, training-efficient, and heterogeneity-tolerant
 071 solution for federated LLM adaptation across mobile devices.

072 Our salient contributions are summarized as follows:

- 073 • We propose Fed MobiLLM, a novel framework that pioneers mobile-friendly, asynchronous
 074 server-assisted side-tuning for LLM adaptation across distributed mobile data. Our design
 075 decouples computation by having devices perform only forward passes (no backpropagation)
 076 and upload activations, where the server asynchronously updates a unified side-network
 077 per-client activation arrival. This eliminates synchronization bottlenecks and removes all
 078 gradient computation from devices.
- 079 • We design adaptive mechanisms enabling Fed MobiLLM to support heterogeneous mobile
 080 devices via capacity-scaled backbone models and cross-architecture layer alignment tech-
 081 niques. This ensures devices with divergent model structures/sizes can collaboratively train
 082 a unified server-side shared side-network that consolidates knowledge from all devices.
- 083 • We implement and evaluate Fed MobiLLM across diverse mobile platforms (NVIDIA Jetson
 084 TX2, Xavier NX, and AGX Xavier) and model scales (sub-billion to billion parameters).
 085 Experiments across multiple tasks and system settings demonstrate that Fed MobiLLM
 086 achieves extremely low on-device memory usage, with at least 95.2% reduction in com-
 087 putation overhead, 93.2% reduction in communication costs and 5.1 \times faster convergence
 088 compared to existing methods. It also delivers state-of-the-art and highly robust LLM
 089 fine-tuning performance.

090 2 RELATED WORK

092 2.1 FEDERATED LLM FINE-TUNING

094 The limited scale and diversity of data on individual mobile devices necessitate collaborative LLM
 095 fine-tuning across devices to enhance model performance. FL has emerged as a dominant paradigm
 096 for this purpose, where devices perform local training and upload parameter updates to a central server
 097 for aggregation. However, fine-tuning large language models (LLMs) under this paradigm presents
 098 significant challenges due to their substantial computational and memory requirements. To address
 099 these constraints, PEFT methods have been widely adopted for local training (Zhang et al., 2023).
 100 Techniques such as Adapters (Houlsby et al., 2019), LoRA (Hu et al., 2022), and BitFit (Zaken et al.,
 101 2021) freeze pretrained backbone parameters while fine-tuning only minimal additional parameters.
 102 To further alleviate on-device memory burden, split federated learning (SFL) approaches further
 103 reduce device load by offloading deeper layers to the server (Tian et al., 2022; Chen et al., 2025;
 104 Gupta & Raskar, 2018). Specifically, devices sequentially exchange activations/gradients with the
 105 server during forward/backward passes, while the device-side sub-models require periodic weight
 106 aggregations across devices. Alternatively, forward-only methods like FwdLLM (Xu et al., 2024)
 107 eliminate backpropagation by estimating gradients through parameter perturbations. While reducing
 108 activation memory to inference levels, this approach requires multiple forward passes per update -
 109 increasing device computational overhead.

108 2.2 EFFICIENT ON-DEVICE LLM FINE-TUNING
109

110 Enabling LLM fine-tuning directly on mobile
111 devices requires innovative architectures that
112 minimize memory and computational load while
113 retaining raw data locally. Server-assisted side-
114 tuning, pioneered by MobiLLM (Li et al., 2025),
115 addresses this by decoupling trainable side-
116 networks from frozen backbones and offloading
117 all the gradient computation to the server. Adv-
118 ancing this approach, PAE MobiLLM (Yang
119 et al., 2025)(as illustrated in Fig. 1) introduces
120 key optimizations: mobile devices perform only
121 a single forward pass through frozen backbones,
122 compute output deviations $\Delta y = \text{Label}_y - y_{\text{pre}}$ without exposing ground-truth labels, and upload
123 selected sparse intermediate activations ($\mathbf{A}_1, \dots, \mathbf{A}_L$) alongside Δy . The server then trains the
124 side-network exclusively using these activation-deviation pairs ($\mathbf{A}_1, \dots, \mathbf{A}_L, \Delta y$), ensuring no raw
125 data access. A server-cached replay mechanism further reduces device overhead by limiting local
126 data processing to the first epoch, with subsequent iterations handled server-side. This achieves an
127 efficient balance between device resource consumption, communication costs, and training speed for
128 on-device LLM fine-tuning. While highly effective for single-device scenarios, scaling server-assisted
129 side-tuning to federated environments introduces fundamental new challenges, including coordination
130 across heterogeneous devices and cross-architecture knowledge aggregation. Our work addresses
131 this gap by extending the side-tuning paradigm to federated fine-tuning scenarios through novel
132 architectural and algorithmic innovations.

132 3 MOTIVATION
133135 3.1 INEFFICIENCIES OF SOTA FEDERATED LLM FT
136

137 State-of-the-art federated LLM fine-tuning methods fail to adequately address the tension between
138 mobile device constraints and LLM computational demands. PEFT techniques reduce communication
139 costs by updating only small modules (e.g., adapters, low-rank matrices), yet still require devices to
140 perform backpropagation through full LLMs. This necessitates storing intermediate activations for
141 all layers during fine-tuning, resulting in memory footprints that significantly exceed typical mobile
142 device capacities - often causing out-of-memory failures or impractical computation delays. Split
143 federated learning mitigates device load by offloading deeper layers to the server but introduces
144 coordination bottlenecks: devices must serially exchange activations and gradients with the server
145 during forward/backward passes, while device-side sub-models require periodic cross-device weight
146 aggregation. In addition, in scenarios where the backbone model is privately deployed within
147 a closed device cluster and is not publicly available, sharing its parameters with the server may
148 violate confidentiality requirements. Forward-only perturbation methods (e.g., FwdLLM) avoid
149 backpropagation at the cost of increased computational overhead, requiring multiple forward passes
150 per update to estimate gradients. Collectively, existing federated LLM fine-tuning approaches exhibit
151 critical gaps and cannot simultaneously optimize on-device memory usage, computational overhead,
152 communication cost, and fine-tuning performance.

152 3.2 HETEROGENEITY CHALLENGES FOR FEDERATED LLM FT
153

154 The significant variation in computational power, memory capacity, and network bandwidth across
155 mobile devices introduces fundamental limitations to traditional synchronous federated learning
156 protocols, which require the central server to wait for model updates from all participating devices
157 before every-round global aggregation. This synchronization barrier creates unavoidable delays
158 caused by slow devices (stragglers), forcing faster devices to remain idle during waiting periods. When
159 applied to LLM fine-tuning, this synchronization bottleneck is exacerbated: intensive computational
160 demands further amplify performance gaps between high- and low-end devices, leaving powerful
161 ones underutilized or idle for extended periods and significantly slowing overall progress. Moreover,
162 memory heterogeneity also leads to significant resource waste. To enable cross-device parameter

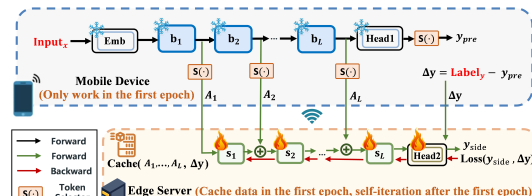


Figure 1: An overview of the PAE MobiLLM.

162 aggregation, all devices must adopt the same backbone model, forcing its size to conform to the
 163 memory constraints of the least-capable device (Su et al., 2024). This constraint underutilizes
 164 the capacity of high-resource devices and results in computational waste. In practice, capable
 165 devices naturally prefer to load larger, more powerful models for achieving better performance. In
 166 summary, as device diversity increases, this inefficiency fundamentally conflicts with FL’s core goal
 167 of collaborative resource utilization, and necessitates asynchronous paradigm designs resilient to
 168 device heterogeneity in computation and memory.

170 4 FED MOBILLM DESIGN

172 4.1 FED MOBILLM OVERVIEW AND PROCEDURE

174 Fed MobiLLM is a server-assisted distributed learning framework designed to enable resource-
 175 constrained mobile devices to collaboratively fine-tune LLMs using their local data. Fig. 2(a) presents
 176 an overview of the Fed MobiLLM system. The key idea is to let devices retain merely a frozen
 177 LLM backbone with pre-trained parameters locally while deploying a tunable side network on the
 178 server. This distinguishes it fundamentally from conventional federated FT approaches that require
 179 full LLMs (frozen backbone + tunable modules) on each device. Fed MobiLLM coordinates devices
 180 to extract features from local data via forward propagation through their frozen backbones, guiding
 181 the server-side training of a shared side-network. By centralizing all tunable parameters on the server,
 182 Fed MobiLLM eliminates expensive on-device backpropagation and reduces memory overhead
 183 (activations/optimizer states) during LLM fine-tuning.

184 During federated tuning, each mobile device performs forward propagation through its frozen
 185 backbone using mini-batches sampled from its local dataset. For each mini-batch, device i transmits
 186 selected intermediate activations ($\mathbf{A}_i^1, \dots, \mathbf{A}_i^L$) from the backbone layers, along with the prediction
 187 residual Δy_i (defined as the difference between ground-truth label and backbone output) to the
 188 server, consistent with PAE MobiLLM’s design (Yang et al., 2025). Upon receiving these activation-
 189 deviation pairs ($\mathbf{A}_i^1, \dots, \mathbf{A}_i^L, \Delta y_i$) from any device, the server updates the shared side-network
 190 immediately, i.e., processing each device’s contribution sequentially upon arrival without global
 191 synchronization¹. As device-side local models are frozen, Fed MobiLLM inherently yields the
 192 following advantages: i) Devices can perform local computations and upload activations at the same
 193 time. ii) Devices keep processing their local data without stopping to wait for server-side updates.
 194 iii) The server triggers immediate side-network updates upon receiving any device’s activations,
 195 eliminating global synchronization barriers. iv) Each device processes its local dataset in just a single
 196 pass during the entire training process. Particularly, the server caches received activations to construct
 197 an activation repository for iterative side-network training. To mitigate non-IID data bias, cached
 198 samples are randomly shuffled during storage. During idle periods, the server trains continuously on
 199 cached samples to maximize computational efficiency. This design ensures uninterrupted training
 200 despite slow devices—eliminating straggler bottlenecks while maintaining full utilization of server
 201 resources. After all devices complete uploading, the server performs efficient standalone tuning
 202 using the comprehensive cached dataset. Through flexible and non-blocking device-server parallel
 203 collaboration, Fed MobiLLM eliminates training bottlenecks and progress stalls caused by slower
 204 devices. (A more detailed description of Fed MobiLLM’s training procedure under heterogeneous
 205 devices is provided in Appendix B.)

206 4.2 HETEROGENEITY-AWARE CROSS-MODEL ALIGNMENT

207 Beyond computational heterogeneity through non-blocking device-server collaboration, Fed Mo-
 208 biLLM fundamentally resolves memory-driven model capacity divergence across mobile devices
 209 where deployable backbone sizes are dictated by each device’s memory constraints. Specifically, Fed
 210 MobiLLM allows each device to load a pre-trained backbone model scaled to its hardware capacity.

211 ¹Note that the concerns about data privacy arising from the transmission of intermediate activations in Fed
 212 MobiLLM are aligned with the definitions adopted in Google’s federated learning (FL) work (McMahan et al.,
 213 2017) and split learning related architectures (Tian et al., 2022). Similar to these approaches, Fed MobiLLM is
 214 naturally compatible with existing advanced privacy-preserving techniques, such as differential privacy (DP)
 215 mechanisms (Dwork, 2006) (e.g., adding DP noise to gradients, inputs, outputs, or objective functions) and
 216 secure multiparty computation (Du & Atallah, 2001).

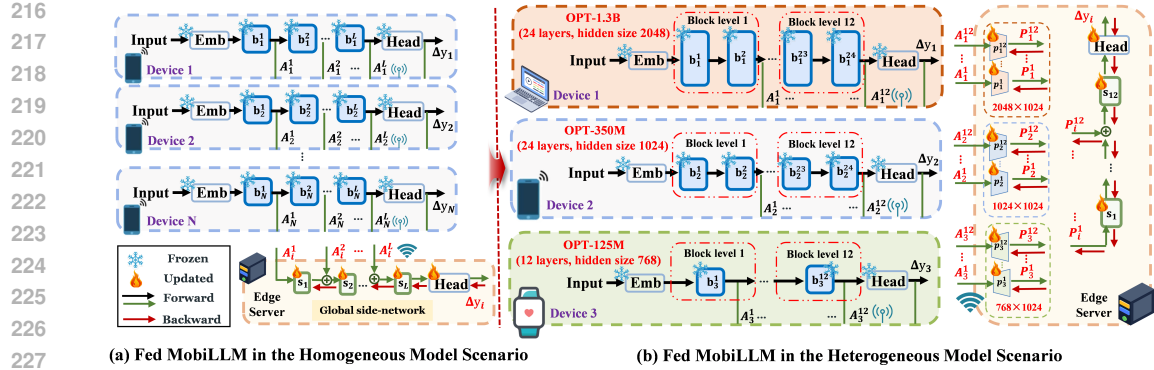


Figure 2: An overview of the Fed MobiLLM.

As illustrated in Fig. 2(b), devices may employ different-sized models (e.g., OPT-125M, OPT-350M, OPT-1.3B (Zhang et al., 2022)), resulting in backbone architectures with varying numbers of transformer layers and hidden dimensions. This architectural diversity introduces two key challenges: (1) server-side adapters must accommodate diverse backbone structures, and (2) uploaded activations exhibit inconsistent shapes across devices. To resolve these issues, we introduce two structural alignment mechanisms—layer-wise activation sampling and hidden dimension scaling—that unify activation patterns across heterogeneous devices for federated training of the shared side-network on the server.

Layer-Wise Activation Sampling. Our layer-wise activation sampling mechanism addresses mismatches in transformer layer counts across backbone models. Inspired by empirical evidence in LST (Sung et al., 2022) demonstrating that not all layers require dedicated adaptation modules, we propose selectively extracting activations from strategic layer positions.

As shown in Fig. 2(b), when devices use backbones with differing layer counts (e.g., 12 vs. 24 layers), we partition all models into a fixed number of blocks (e.g., 12 blocks). Activations are then sampled exclusively from the final layer of each block. The server-side network is configured with an equal number of adapter modules, each processing one aligned activation block. Through comparative experiments of various strategies, we established optimal configuration guidelines: the block count is set to the minimum layer depth among participating models (e.g., 12 blocks for 12/24-layer models), while deeper models are partitioned at uniform intervals (e.g., sampling every other layer in a 24-layer backbone). This approach ensures layer-wise structural consistency while preserving representational capacity.

Hidden Size Scaling. Pre-trained models of different scales exhibit varying hidden sizes, preventing direct integration of their activations into a unified side-network adapter module. To resolve this, we introduce dedicated trainable linear projection layers for each backbone model type, mapping activations to a consistent hidden size for shared side-network processing.

As shown in Fig. 2(b), three distinct backbone models (hidden sizes: 2048, 1024, 768) require dimension standardization. We configure the side-network adapter with a target hidden size of 1024 and deploy projection layers (p_i^1, \dots, p_i^{12}) on the server for each model variant. Consider device 1 using OPT-1.3B (hidden size 2048): its activations (A_1^1, \dots, A_1^{12}) pass through corresponding projection layers ($p_1^1, \dots, p_1^{12} \in \mathbb{R}^{2048 \times 1024}$), producing transformed activations (P_1^1, \dots, P_1^{12}) with uniform 1024-dimensional features. These standardized activations then feed into the shared adapter modules (s_1^1, \dots, s_1^{12}), which enable collaborative training across heterogeneous models.

All projection layers are server-managed and co-trained with the side-network. After fine-tuning, devices download their specific projection layers alongside the shared side-network for local inference. Our empirical study suggests selecting mid-range dimensions (e.g., 1024 for 768/1024/2048 scenarios) can optimize efficiency-accuracy balance in multi-device scenarios, while prioritizing larger dimensions can preserve representation capacity in scenarios involving only two model sizes.

270 5 EXPERIMENTAL SETUP
271272 5.1 FED MOBILLLM IMPLEMENTATION
273

274 The experimental testbed consists of a server with an NVIDIA A100 GPU and three types of
275 heterogeneous client devices representing increasing computational capabilities for LLM processing:
276 (1) NVIDIA Jetson TX2 (8GB RAM, 1.3 TFLOPS), (2) NVIDIA Jetson Xavier NX (8GB RAM, 6
277 TFLOPS peak), and (3) NVIDIA Jetson AGX Xavier (16GB RAM, up to 10 TFLOPS peak).

278 5.2 MODELS, DATASETS AND PARAMETERS
279

280 **Models:** To systematically evaluate Fed MobiLLM’s performance, we employ two representative
281 pre-trained LLM architectures: i) decoder-based OPT series (OPT-1.3B, OPT-350M, OPT-125M),
282 and ii) encoder-based RoBERTa series (RoBERTa-large(350M) and RoBERTa-base(125M)). This
283 selection ensures architectural diversity while maintaining mobile compatibility. All models are
284 initialized via HuggingFace Transformers (Wolf et al., 2019).

285 **Datasets:** We take the GLUE benchmark (Wang et al., 2018) and DialogSum dataset (Chen
286 et al., 2021) for the evaluation of NLP tasks, which are widely used in the fine-tuning research
287 for LLM (Zhang et al., 2023; Sun et al., 2024; Sung et al., 2022). GLUE benchmark comprises
288 eight tasks, including linguistic acceptability (CoLA (Warstadt, 2019)), sentiment analysis (SST-
289 2 (Socher et al., 2013)), similarity and paraphrase (MRPC (Dolan & Brockett, 2005), QQP (Iyer
290 et al., 2017), STS-B (Cer et al., 2017)), and natural language inference (MNLI (Williams et al.,
291 2017), QNLI (Rajpurkar, 2016), RTE (Bentivogli et al., 2009)). DialogSum includes summaries of
292 real-world conversations on a diverse set of topics and scenarios to evaluate text-generation tasks. We
293 use ROUGE scores (R1/R2/RL) as the accuracy metric. Following FedPETuning (Zhang et al., 2023),
294 we simulate non-IID data partitions using a Dirichlet distribution with concentration parameter α ,
295 where lower α values induce higher label distribution shift. (See Appendix C for dataset details.)

296 **Parameters:** Following FedPETuning (Zhang et al., 2023), we set the number of communication
297 rounds to 100 and the number of local training epochs to 1 for all baselines under the FL paradigm.
298 All configurations deploy 100 clients with balanced device-type distribution in heterogeneous settings.
299 For Fed MobiLLM and those centralized fine-tuning baselines, the number of training epochs is set to
300 20. To ensure fair comparison, all experiments share the same configurations unless specified: FP16
301 precision, batch size 8, learning rate 5e-4, maximum sequence length 256, and 60 Mbps in-lab Wi-Fi
302 transmission speed. Additionally, LoRA and Fed MobiLLM employ rank-64 low-rank trainable
303 modules by default, while FwdLLM uses 300 global perturbations per iteration.

304 5.3 BASELINES FOR PERFORMANCE COMPARISON
305

306 We compare Fed MobiLLM with three baseline approaches: i) **FedPETuning** (Zhang et al., 2023)
307 (hereafter **FL**): Implements standard FedAvg aggregation with local PEFT on devices. ii) **Fed-
308 Bert** (Tian et al., 2022) (hereafter **SFL**): Extends FL with split learning, retaining only first/last
309 transformer layers on devices while offloading intermediate layers to the server. iii) **FwdLLM** (Xu
310 et al., 2024): Follows FL paradigm but replaces backpropagation with on-device perturbation training.

311 Each baseline is evaluated with two representative PEFT methods: i) **LoRA** (Hu et al., 2022): Inserts
312 trainable low-rank matrices into frozen backbone networks. ii) **BitFit** (Zaken et al., 2021): Fine-tunes
313 exclusively bias terms while freezing other pre-trained weights.

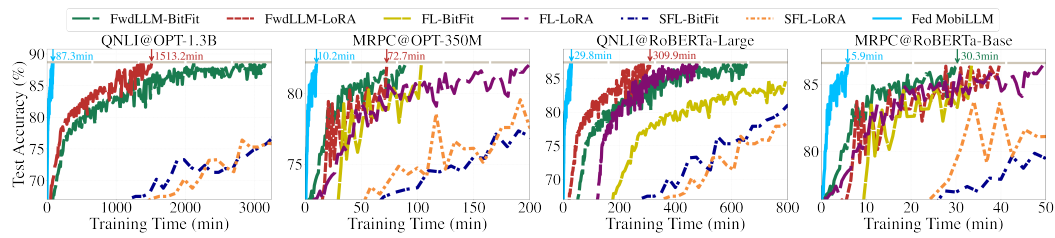
315 6 EVALUATION RESULTS AND ANALYSIS
316317 6.1 COMPARATIVE ANALYSIS WITH FEDERATED FT BASELINES
318

319 We conduct comprehensive experiments to validate Fed MobiLLM’s advantages in on-device resource
320 efficiency, training efficiency, and fine-tuning performance across homogeneous and heterogeneous
321 device environments. (See Appendix D for details of result computation.)

322 **On-Device Resource Efficiency.** As detailed in Table 1, Fed MobiLLM demonstrates superior
323 resource efficiency across metrics in terms of on-device memory footprint, computation cost, and

324
 325 Table 1: Comparison across methods: i) Per-device resource efficiency (mem-
 326 ory/computation/communication); ii) Fine-tuning accuracy (centralized training vs. federated
 327 training); and iii) Time-to-Accuracy (TTA) under homogeneous (TX2/Xavier/AGX Xavier clusters)
 328 and heterogeneous (Mixed) device configurations. Task: RoBERTa-Base@MRPC. Note: *Fed*
MobiLLM uses uniform backbone models across devices in mixed settings for fairness.

Methods	On-device memory (GB)	On-device comp. (TFLOPs)	On-device comm. (MB)	FT Performance (Acc.)		TTA@86.5(Mins)			
				Centralized	Federated	TX2 (Hom.)	Xavier (Hom.)	AGX (Hom.)	Mixed (Heter.)
FL-LoRA	1.18	395.7	31.1	91.5	86.9	54.2	41.6	35.7	49.3
FL-BitFit	1.02	388.1	23.1	90.7	86.8	49.7	39.1	32.2	35.6
SFL-LoRA	0.54	58.3	5437.5	91.5	87.8	782.1	763.2	741.3	777.3
SFL-BitFit	0.49	56.5	5429.4	90.7	87.2	774.2	751.2	722.9	767.9
FwdLLM-LoRA	0.42	407.4	22.8	91.5	87.1	41.2	28.9	25.4	40.3
FwdLLM-BitFit	0.38	391.5	16.2	90.7	87.4	32.7	22.9	20.2	30.3
Fed MobiLLM	0.38	2.7	1.1	89.6	88.1	5.7	6.0	5.1	5.9



347 Figure 3: Convergence performance on various models and tasks under heterogeneous-device settings.
 348

350 communication cost. Conventional FL-based PEFT methods (e.g., FedPETuning) incur substantial
 351 resource demands, while SFL approaches like FedBert trade computation savings for significantly
 352 increased communication overhead (up to 175 \times). Similarly, FwdLLM trades memory savings for
 353 higher computation load. In contrast, Fed MobiLLM maintains an optimal balance, where devices
 354 perform only a single forward pass, reducing memory consumption to inference levels (e.g., 2.68 \times
 355 reduction for RoBERTa-Base). Besides, it achieves at least 95.2% lower computation and 93.2%
 356 less communication by eliminating on-device backpropagation and leveraging server-side activation
 357 caching.

358 **Training Efficiency.** We evaluate Fed MobiLLM’s training efficiency by measuring time-to-accuracy
 359 across diverse configurations, including two model architectures (OPT, RoBERTa) and two tasks
 360 (MRPC, QNLI), as shown in Fig. 3. To ensure fair comparison, all heterogeneous devices use identical
 361 backbone models across Fed MobiLLM and other baselines. The results show that Fed MobiLLM
 362 achieves at least a 5.1 \times speedup across all tasks. This acceleration stems from our full-pipeline
 363 efficient design: during the initial phase, clients perform only one forward propagation per data
 364 sample, avoiding both on-device backpropagation in conventional FL and multi-pass perturbations in
 365 FwdLLM. After aggregating activations from all devices, the server performs iterative training on the
 366 shared side-network independently, eliminating parameter synchronization with devices inherent in
 367 FL paradigms.

368 We further evaluate training efficiency across different client device setups, as shown in Table 1, which
 369 validates Fed MobiLLM’s superior straggler resilience. Under the heterogeneous-device setting,
 370 baselines suffer severe slowdowns due to synchronous waiting periods in federated aggregation
 371 protocols, resulting in training times approaching the all-TX2 (lowest-capacity devices) configuration.
 372 In contrast, Fed MobiLLM benefits from extremely lightweight on-device computation and non-
 373 blocking parallel device-server collaboration. As a result, computational speed variations across
 374 devices are effectively masked, yielding consistent training times across diverse client setups.

375 **LLM FT Performance.** We evaluate Fed MobiLLM against federated LLM FT methods and their
 376 centralized PEFT counterparts (LoRA, BitFit, side-network tuning). As Table 1 shows, while LoRA
 377 and BitFit outperform side-network tuning in centralized settings, their accuracy significantly degrades
 under federated deployment with distributed data. Even the best federated baseline (FwdLLM-BitFit)

378
379Table 2: FT Performance under data heterogeneity: IID vs. non-IID ($\alpha = \{0.1, 1.0, 10.0\}$).380
381
382
383
384
385
386
387
388

Methods	RoBERTa-Base@MRPC (Acc.)			OPT-1.3B@DialogSum (R1/R2/RL)			
	IID	non-IID ($\alpha = 10.0$)	non-IID ($\alpha = 1.0$)	non-IID ($\alpha = 0.1$)	IID	non-IID ($\alpha = 10.0$)	non-IID ($\alpha = 0.1$)
FL-LoRA	86.9	85.1	84.5	82.1	19.2 / 6.1 / 15.1	17.9 / 5.2 / 14.3	16.1 / 4.6 / 12.7
FL-BitFit	86.8	84.9	84.6	81.5	19.0 / 6.2 / 14.9	17.7 / 5.1 / 14.2	16.4 / 4.2 / 12.9
SFL-LoRA	87.8	87.1	86.8	84.3	19.9 / 6.5 / 15.8	18.5 / 6.1 / 15.1	18.0 / 5.5 / 13.8
SFL-BitFit	87.2	87.0	86.1	85.2	19.7 / 6.2 / 15.5	18.7 / 6.0 / 15.2	17.8 / 5.4 / 13.4
FwdLLM-LoRA	87.1	86.7	86.5	84.1	19.3 / 6.3 / 15.7	18.2 / 6.2 / 15.1	17.8 / 5.2 / 13.7
FwdLLM-BitFit	87.4	87.1	86.6	84.7	19.6 / 5.9 / 15.1	18.6 / 6.1 / 14.9	17.3 / 5.1 / 14.1
Fed MobiLLM	88.1	87.8	87.7	87.3	21.0 / 7.7 / 17.2	20.2 / 7.4 / 16.0	20.0 / 7.3 / 16.3

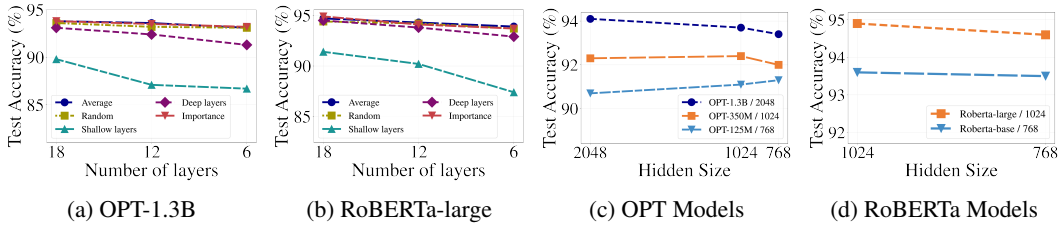
389
390
391
392
393
394
395396
397
398
399

Figure 4: Comparative accuracy across sampling methods (a-b) and hidden-size scaling (c-d) (Task: SST-2).

400
401
402
403
404
405
406
407
408
409

exhibits at least 3.3% performance drop. In contrast, Fed MobiLLM maintains near-centralized with only a 1.5% accuracy drop, outperforming all federated FT baselines by at least 0.3%.

We further evaluate the impacts of data heterogeneity on Fed MobiLLM’s performance. To build local datasets, we use three Dirichlet distributions ($\alpha \in \{0.1, 1.0, 10.0\}$) where a lower α indicates a higher non-IID level (Zhang et al., 2023). Table 2 demonstrates that while the performance of all methods degrades under data heterogeneity, Fed MobiLLM shows superior resilience. Taking the MRPC task as an example, at extreme heterogeneity ($\alpha = 0.1$), Fed MobiLLM’s accuracy drop is 1.2% smaller than SFL-BitFit, validating enhanced robustness to cross-client data distribution shifts.

410
411

6.2 CROSS-MODEL ALIGNMENT PERFORMANCE

412
413
414

We evaluate the efficacy of our layer-wise activation sampling and hidden size scaling methods for heterogeneous model adaptation through comparative experiments with alternative approaches.

415
416
417
418
419
420
421
422
423

Layer Alignment Design. To determine optimal block configurations for layer alignment in Fed MobiLLM, we perform comparative experiments using OPT-1.3B and RoBERTa-Large models. Specifically, we feed sampled layer-wise backbone activations to the side network and analyze how layer-wise activation sampling strategies affect performance, as shown in Fig. 4 (a-b). We compare five strategies: shallow-only, deep-only, average-interval, random, and importance-based selection (identified via layer-wise ablation). Results indicate: i) Performance improves with more backbone activation layers; ii) The average-interval strategy achieves accuracy comparable to computationally intensive importance-based approaches. These findings support Fed MobiLLM’s configuration: set block count to the most lightweight LLM backbone’s layer depth across devices, partitioning larger-sized LLMs at equal intervals to ensure structural alignment while maintaining performance.

424
425
426
427
428
429
430
431

Hidden Size Alignment Design. For cross-model hidden size scaling, determining a unified dimension for side-network adapters is critical. We experiment with various OPT and RoBERTa models, and evaluate performance under different side-network hidden sizes. As shown in Fig. 4 (c-d), peak performance is achieved when side-network hidden sizes match backbone sizes, while dimensional mismatches degrade accuracy. For example, OPT-125M (hidden size = 768) performs worse when forced dimension to 2048, which demonstrates that larger dimensions aren’t always beneficial. These findings yield practical Fed MobiLLM configuration guidelines: for multi-device scenarios, select median dimensions (e.g., 1024 for 768/1024/2048); for dual-model scenarios, prioritize larger dimensions to preserve representational capacity.

432 Table 3: Fed MobiLLM under heterogeneous device configurations with capacity-scaled backbone
 433 allocation. (*Single*: isolated side-network training on each single device’s local data; *Global*:
 434 collaborative training of a shared side-network. Results partitioned by model family (OPT series
 435 upper, RoBERTa series lower) on SST-2 task.)

Devices	Local Backbone Model	On-device Memory (GB)	On-device Comp. (TFLOPs)	Per-device Local Runtime(s)	FT Performance (Acc.)					
					IID		$(\alpha=1.0)$		$(\alpha=0.1)$	
Single	Global	Single	Global	Single	Global					
AGX	OPT-1.3B	3.44	422.3	92.3	90.0	92.9	89.1	92.3	83.1	91.9
Xavier	OPT-350M	1.10	108.8	88.2	89.9	92.4	88.5	91.8	81.6	91.5
TX2	OPT-125M	0.56	31.5	84.6	88.4	92.1	87.4	91.6	80.4	91.6
AGX	RoBERTa-large	0.86	108.4	81.9	91.8	93.5	88.1	92.7	84.3	91.7
Xavier	RoBERTa-large	0.86	108.4	92.4	91.8	93.5	88.1	92.7	84.3	91.7
TX2	RoBERTa-base	0.38	30.9	90.7	90.4	92.7	87.6	92.3	82.9	91.0

445 446 447 6.3 VALIDATION OF HETEROGENEOUS BACKBONE ADAPTATION

448 To validate the efficacy and necessity of Fed MobiLLM’s heterogeneous backbone design, we
 449 conduct systematic experiments across OPT and RoBERTa model series, where each device loads a
 450 capacity-scaled backbone model tailored to its hardware capabilities.

451 **Device-Specific Workload Balancing.** As shown in the results of the on-device workload in
 452 Table 3, device-specific backbone assignment optimizes hardware resource utilization compared to
 453 uniform model deployment. For example, AGX Xavier and Xavier run OPT-1.3B and OPT-350M,
 454 respectively, with memory usage both around 30% of their available capacities (12.4 GB and 4.6 GB).
 455 Computational loads similarly scale to device capacities, resulting in comparable execution times for
 456 local forward propagation and activation uploads across heterogeneous devices. This helps ensure
 457 near-balanced contributions to side-network training and prevent representation drift toward data
 458 from those fast devices. This confirms Fed MobiLLM’s effective workload balancing and cross-client
 459 coordination through hardware-aware model scaling.

460 **Cross-Capacity Collaboration Effects.** We investigate whether collaboration with lower-capacity
 461 devices in Fed MobiLLM compromises high-capacity device performance. To this end, we evaluate
 462 performance under two settings: i) training the side network using only each device’s local data
 463 (denoted by *Single*), and ii) federated training of a shared side network across all devices (denoted
 464 by *Global*). As shown in Table 3, *Global* consistently outperforms *Single* across different backbone
 465 sizes and data distributions, particularly under high data heterogeneity. For example, when $\alpha =$
 466 0.1, the accuracy improvement is at least 8.8% and 7.4% with OPT models and RoBERTa models,
 467 respectively. These results demonstrate that Fed MobiLLM enables all devices to benefit from
 468 collaboratively trained robust side-networks without performance degradation.

471 7 CONCLUSION

472 This paper has presented Fed MobiLLM, an efficient and scalable framework for federated fine-tuning
 473 of LLMs across heterogeneous mobile devices. By pioneering an asynchronous server-assisted side-
 474 tuning paradigm, Fed MobiLLM decouples device responsibilities to forward-only propagation and
 475 activation uploading, while the server trains a shared side-network, which eliminates synchronization
 476 bottlenecks inherent in conventional FL-based fine-tuning approaches. Through layer-wise activation
 477 sampling and cross-architecture dimension alignment, Fed MobiLLM enables each device to load
 478 backbone models that match its hardware capacities while still maintaining the ability to collabora-
 479 tively train a shared side network, ensuring robust support for device heterogeneity. Extensive
 480 experiments demonstrate Fed MobiLLM’s efficacy and efficiency: achieving 2.68 \times reduction in
 481 on-device memory usage, 95.2% reduction in computational cost, 93.2% lower communication
 482 overhead, and 5.1 \times faster convergence compared to state-of-the-art methods, while maintaining
 483 competitive accuracy under IID/non-IID data distributions. These results collectively establish Fed
 484 MobiLLM as a practical and deployment-ready solution for real-world federated LLM fine-tuning on
 485 distributed mobile datasets. (See Appendix E for extended discussion.)

486 8 REPRODUCIBILITY STATEMENT

488 It is important to note that the work presented in this paper is reproducible. To ensure the reproducibility
 489 of our results, we have made several efforts, which we summarize below. A detailed description
 490 of our method is provided in Section 4 and Appendix B. Comprehensive implementation details,
 491 encompassing hyperparameter configurations and optimization procedures, are delineated in Sec-
 492 tion 5 and Appendix D. For reproducibility, the source code has been included in the supplementary
 493 materials. Following acceptance, it will be released publicly on GitHub to facilitate further research.
 494 By providing these detailed resources, we aim to ensure that our work can be reproduced accurately.
 495 Furthermore, we encourage others to conduct further exploration and research based on our work.

497 REFERENCES

499 Luisa Bentivogli, Peter Clark, Ido Dagan, and Danilo Giampiccolo. The fifth pascal recognizing
 500 textual entailment challenge. *TAC*, 7(8):1, 2009.

501 Tom Brown, Benjamin Mann, Nick Ryder, Melanie Subbiah, Jared D Kaplan, Prafulla Dhariwal,
 502 Arvind Neelakantan, Pranav Shyam, Girish Sastry, Amanda Askell, et al. Language models are
 503 few-shot learners. *Advances in neural information processing systems*, 33:1877–1901, 2020.

505 Daniel Cer, Mona Diab, Eneko Agirre, Inigo Lopez-Gazpio, and Lucia Specia. Semeval-2017 task
 506 1: Semantic textual similarity-multilingual and cross-lingual focused evaluation. *arXiv preprint*
 507 *arXiv:1708.00055*, 2017.

508 Xiaopei Chen, Liang Li, Fei Ji, and Wen Wu. Memory-efficient split federated learning for llm
 509 fine-tuning on heterogeneous mobile devices. *arXiv preprint arXiv:2506.02940*, 2025.

511 Yulong Chen, Yang Liu, Liang Chen, and Yue Zhang. Dialogsum: A real-life scenario dialogue
 512 summarization dataset. *arXiv preprint arXiv:2105.06762*, 2021.

514 Jacob Devlin, Ming-Wei Chang, Kenton Lee, and Kristina Toutanova. Bert: Pre-training of deep
 515 bidirectional transformers for language understanding. *arXiv preprint arXiv:1810.04805*, 2018.

516 Bill Dolan and Chris Brockett. Automatically constructing a corpus of sentential paraphrases. In
 517 *Third international workshop on paraphrasing (IWP2005)*, 2005.

519 Wenliang Du and Mikhail J Atallah. Secure multi-party computation problems and their applications:
 520 a review and open problems. In *Proceedings of the 2001 workshop on New security paradigms*, pp.
 521 13–22, 2001.

523 Cynthia Dwork. Differential privacy. In *International colloquium on automata, languages, and*
 524 *programming*, pp. 1–12. Springer, 2006.

525 Otkrist Gupta and Ramesh Raskar. Distributed learning of deep neural network over multiple agents.
 526 *Journal of Network and Computer Applications*, 116:1–8, 2018.

528 Neil Houlsby, Andrei Giurgiu, Stanislaw Jastrzebski, Bruna Morrone, Quentin De Laroussilhe,
 529 Andrea Gesmundo, Mona Attariyan, and Sylvain Gelly. Parameter-efficient transfer learning for
 530 nlp. In *Proc. of 36th International Conference on Machine Learning (ICML)*, Long Beach, CA,
 531 June 2019.

532 Edward J Hu, Yelong Shen, Phillip Wallis, Zeyuan Allen-Zhu, Yuanzhi Li, Shean Wang, Lu Wang,
 533 Weizhu Chen, et al. Lora: Low-rank adaptation of large language models. *ICLR*, 1(2):3, 2022.

535 Shankar Iyer, Nikhil Dandekar, Kornél Csernai, et al. First quora dataset release: Question pairs.
 536 *data. quora. com*, 2017.

538 Liang Li, Xingke Yang, Wen Wu, Hao Wang, Tomoaki Ohtsuki, Xin Fu, Miao Pan, and Xuemin Shen.
 539 Mobillm: Enabling llm fine-tuning on the mobile device via server assisted side tuning. *arXiv*
preprint arXiv:2502.20421, 2025.

540 Brendan McMahan, Eider Moore, Daniel Ramage, Seth Hampson, and Blaise Aguera y Arcas.
 541 Communication-efficient learning of deep networks from decentralized data. In *Artificial intelligence and statistics*, pp. 1273–1282. PMLR, 2017.
 542

543 P Rajpurkar. Squad: 100,000+ questions for machine comprehension of text. *arXiv preprint arXiv:1606.05250*, 2016.

544

545 Xubin Ren, Wei Wei, Lianghao Xia, Lixin Su, Suqi Cheng, Junfeng Wang, Dawei Yin, and Chao Huang. Representation learning with large language models for recommendation. In *Proceedings of the ACM Web Conference 2024*, pp. 3464–3475, 2024.

546

547 Richard Socher, Alex Perelygin, Jean Wu, Jason Chuang, Christopher D Manning, Andrew Y Ng, and Christopher Potts. Recursive deep models for semantic compositionality over a sentiment treebank.
 548 In *Proceedings of the 2013 conference on empirical methods in natural language processing*, pp.
 549 1631–1642, 2013.

550

551 Huai-an Su, Pavana Prakash, Rui Chen, Yanmin Gong, Rong Yu, Xin Fu, and Miao Pan. Dafl:
 552 Device-to-device transmissions for delay efficient federated learning over mobile devices. *IEEE Internet of Things Journal*, 2024.

553

554 Youbang Sun, Zitao Li, Yaliang Li, and Bolin Ding. Improving lora in privacy-preserving federated
 555 learning. *arXiv preprint arXiv:2403.12313*, 2024.

556

557 Yi-Lin Sung, Jaemin Cho, and Mohit Bansal. Lst: Ladder side-tuning for parameter and memory
 558 efficient transfer learning. In *Proc. of Advances in Neural Information Processing Systems (NeurIPS)*, New Orleans, Louisiana, December 2022.

559

560 Yuanyishu Tian, Yao Wan, Lingjuan Lyu, Dezhong Yao, Hai Jin, and Lichao Sun. Fedbert: When
 561 federated learning meets pre-training. *ACM Transactions on Intelligent Systems and Technology (TIST)*, 13(4):1–26, 2022.

562

563 Hugo Touvron, Thibaut Lavril, Gautier Izacard, Xavier Martinet, Marie-Anne Lachaux, Timothée
 564 Lacroix, Baptiste Rozière, Naman Goyal, Eric Hambrø, Faisal Azhar, et al. Llama: Open and
 565 efficient foundation language models. *arXiv preprint arXiv:2302.13971*, 2023.

566

567 Alex Wang, Amanpreet Singh, Julian Michael, Felix Hill, Omer Levy, and Samuel R Bowman.
 568 Glue: a multi-task benchmark and analysis platform for natural language understanding. *corr abs/1804.07461* (2018). *arXiv preprint arXiv:1804.07461*, 2018.

569

570 A Warstadt. Neural network acceptability judgments. *arXiv preprint arXiv:1805.12471*, 2019.

571

572 Adina Williams, Nikita Nangia, and Samuel R Bowman. A broad-coverage challenge corpus for
 573 sentence understanding through inference. *arXiv preprint arXiv:1704.05426*, 2017.

574

575 Thomas Wolf, Lysandre Debut, Victor Sanh, Julien Chaumond, Clement Delangue, Anthony Moi,
 576 Pierrick Cistac, Tim Rault, Rémi Louf, Morgan Funtowicz, et al. Huggingface’s transformers:
 577 State-of-the-art natural language processing. *arXiv preprint arXiv:1910.03771*, 2019.

578

579 Mengwei Xu, Dongqi Cai, Yaozong Wu, Xiang Li, and Shangguang Wang. {FwdLLM}: Efficient
 580 federated finetuning of large language models with perturbed inferences. In *2024 USENIX Annual
 581 Technical Conference (USENIX ATC 24)*, pp. 579–596, 2024.

582

583 Xingke Yang, Liang Li, Zhiyi Wan, Sicong Li, Hao Wang, Xiaoqi Qi, Jiang Liu, Tomoaki Ohtsuki,
 584 Xin Fu, and Miao Pan. Pae mobillm: Privacy-aware and efficient llm fine-tuning on the mobile
 585 device via additive side-tuning. *arXiv preprint arXiv:2507.01216*, 2025.

586

587 Qinyuan Ye. Cross-task generalization abilities of large language models. In *Proceedings of the
 588 2024 Conference of the North American Chapter of the Association for Computational Linguistics:
 589 Human Language Technologies (Volume 4: Student Research Workshop)*, pp. 255–262, 2024.

590

591 Elad Ben Zaken, Shauli Ravfogel, and Yoav Goldberg. Bitfit: Simple parameter-efficient fine-tuning
 592 for transformer-based masked language-models. *arXiv preprint arXiv:2106.10199*, 2021.

593

594 Susan Zhang, Stephen Roller, Naman Goyal, Mikel Artetxe, Moya Chen, Shuohui Chen, Christopher
595 Dewan, Mona Diab, Xian Li, Xi Victoria Lin, et al. Opt: Open pre-trained transformer language
596 models. *arXiv preprint arXiv:2205.01068*, 2022.

597
598 Zhuo Zhang, Yuanhang Yang, Yong Dai, Qifan Wang, Yue Yu, Lizhen Qu, and Zenglin Xu. Fed-
599 petuning: When federated learning meets the parameter-efficient tuning methods of pre-trained
600 language models. In *Annual Meeting of the Association of Computational Linguistics 2023*, pp.
9963–9977. Association for Computational Linguistics (ACL), 2023.

601

602

603

604

605

606

607

608

609

610

611

612

613

614

615

616

617

618

619

620

621

622

623

624

625

626

627

628

629

630

631

632

633

634

635

636

637

638

639

640

641

642

643

644

645

646

647

648 **A LLM USAGE DECLARATION**
649650 Large language models (e.g., ChatGPT) were used solely for language editing and formatting. They
651 did not contribute to the conception, design, implementation, analysis, data generation or labeling, or
652 evaluation of the methods and results. All technical content and claims were authored and verified by
653 the authors, and no personal, proprietary, or sensitive data were shared with LLM services.
654655 **B FED MOBILLLM DETAILED PROCEDURES**
656657 Without loss of generality, we present here a more detailed description of the entire process by which
658 Fed MobiLLM performs LLM fine-tuning for downstream tasks in heterogeneous mobile device
659 scenarios.
660661 **(1) Initialization (on mobile device & server):**662

- 663 Before federated LLM fine-tuning begins, each mobile device loads a pre-trained LLM
664 backbone that matches its local compute and memory budget, chosen based on its inference
665 footprint. Each device then sends the loaded backbone parameters to the server.
- 666 Upon aggregating the configurations of all N participating devices, the server configures
667 the shared side network as follows: (i) set the number of adapter modules to the minimum
668 backbone depth across devices (e.g. 12 blocks for 12/24-layer backbones); (ii) set the adapter
669 hidden size to the median hidden dimension across devices (e.g., 1024 for 768/1024/2048);
670 and (iii) allocate a projection layer P for each backbone hidden size. The adapter modules
671 and projection layers on the server are trainable and initialized from a zero-mean Gaussian
672 distribution with a well-chosen standard deviation.
- 673 The server then communicates the chosen number of shared adapters to all devices (i.e.,
674 the number of blocks to which each device will align). Given its own depth, each device
675 determines which layers to upload by sampling in a block-wise manner at uniform intervals
676 (e.g., every other layer in a 24-layer backbone).

677 **(2) Local backbone forward propagation and activation upload (on mobile device):**
678679

- 680 During training, the N devices run independently. Each device samples a mini-batch from
681 its local dataset and performs forward propagation through the frozen backbone. Following
682 the block-wise selection decided at initialization, the device records activations at the
683 transformer layers designated for upload.
- 684 For each mini-batch, after the forward pass the device obtains the local prediction y_{pre} and
685 computes the deviation from the ground truth y_{label} as $\Delta y = y_{\text{label}} - y_{\text{pre}}$. In parallel, for
686 intermediate activations at each transformer layer, the device extracts only the positions
687 relevant to the current task involved in the calculation of the loss (e.g., the last token in the
688 classification), resulting in the activation set $(\mathbf{A}_i^1, \dots, \mathbf{A}_i^L)$. For a more detailed explanation
689 of Δy and the token selector, refer to PAE MobiLLM (Yang et al., 2025). Once Δy is
690 computed and $(\mathbf{A}_i^1, \dots, \mathbf{A}_i^L)$ is selected, the mini-batch forms an activation-deviation pair
691 $(\mathbf{A}_i^1, \dots, \mathbf{A}_i^L, \Delta y_i)$, which is immediately submitted to the server.
- 692 On each device, training proceeds mini-batch by mini-batch: after completing the forward
693 pass and uploading the activation-deviation pair for a mini-batch, the device immediately
694 moves to the next one. Once the local dataset has been traversed once, the device's local
695 work is complete. In contrast to previous methods that repeatedly iterate over local data
696 until convergence, Fed MobiLLM keeps the device-side backbone frozen and leverages
697 server-side caching and reuse, so the device avoids redundant on-device computation.

698 **(3) Forward and backward propagation training (on server):**
699700

- 701 The server runs in an asynchronous, arrive-and-train manner: it receives activation-deviation
702 pairs from devices and updates the model immediately upon arrival. For each incoming
703 sample, the server first inspects the hidden size of the uploaded activations, applies the
704 corresponding projection layer p in the forward pass, and then runs the shared side-network

(adapters) forward. It computes the loss between the side-network output y_{side} and the deviation Δy , and backpropagates along the same path. As a result, activations from different hidden-size backbones *jointly* train the shared adapters while *separately* updating their size-specific projection layers; activations with the same hidden size *jointly* update the same adapter stack and projection layer.

- After each update, the server also inserts the sample into a cache for replay. To mitigate non-IID bias, cached samples are randomly shuffled at insertion and sampling. During idle periods, the server continues to train on cached samples to maximize compute utilization. This design keeps training uninterrupted despite slow devices, eliminates straggler bottlenecks, and maintains high server utilization.

(4) Fine-tuned side-network download and local inference (server \rightarrow mobile device):

After the federated LLM fine-tuning is complete, the mobile device downloads from the server the **projection layer** p that matches its hidden size and the **side-network (adapters)**, for on-device inference (see Fig. 5). These modules can be seamlessly attached to the frozen local backbone. During inference, the side network produces y_{side} , which provides a residual correction to the backbone output y_{pre} , producing the fine-tuned model output $y_{\text{output}} = y_{\text{pre}} + y_{\text{side}}$. This also clarifies why the server-side training targets the deviation $\Delta y = y_{\text{label}} - y_{\text{pre}}$: by learning to predict Δy , the deployed side-network output y_{side} approximates this deviation, ensuring the residual correction is aligned with the downstream task.

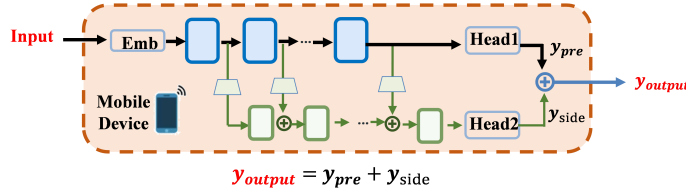


Figure 5: How to execute on-device inferences in Fed MobiLLM.

C DATASETS STATISTICS

Table 4: Datasets Statistics.

Dataset	Description	Task	# Samples (train/eval)
CoLA	Linguistic Acceptability	Classification	8551 / 1043
SST2	Sentiment Analysis	Classification	67350 / 873
MRPC	Sentence Equivalence	Classification	5801 / 408
STSB	Sentence Similarity	Regression	5712 / 1471
QQP	Paraphrase Recognition	Classification	363847 / 40431
RTE	Textual Entailment	Classification	2491 / 278
QNLI	Natural Language Inference	Classification	103141 / 5268
MNLI	Textual Entailment	Classification	392702 / 9815(9832)
DialogSum	Abstract Summary	Generation	12460 / 500

D COMPUTATION OF REPORTED RESULTS

In this section, we use Table 1 as an example to present how we compute *on-device resource overhead* and *training efficiency* metrics for Fed MobiLLM and other baselines. We consider a federated setting with 100 homogeneous NVIDIA Xavier clients, each of which loads the same RoBERTa-Base backbone. The unified experimental setup is as follows: using the MRPC dataset with 5,801 samples, data is evenly distributed across 100 clients (58 samples per client) according to the standard federated learning configuration. FP16 precision, batch size = 8, sequence length = 256, and an in-lab Wi-Fi throughput of 60 Mbps.

756 D.1 ON-DEVICE MEMORY FOOTPRINT
757

758 • **FL-LoRA:** Performs full LoRA fine-tuning on the RoBERTa model on the device. The
759 memory footprint consists of model weights + intermediate activation + optimizer states
760 and hence is the largest among all methods.

761 • **SFL-LoRA (U-shaped split learning):** To keep raw data and labels on the device, only
762 offload the middle 10 layers of the 12-layer transformer to the server; the remaining layers
763 are LoRA fine-tuned on the device. The memory footprint consists of partial weights +
764 partial intermediate activation + partial optimizer states, thus lower than FL-LoRA.

765 • **FwdLLM-LoRA and Fed MobiLLM:** The device only performs forward propagation.
766 The memory footprint consists of model weights + a small inference-time intermediate
767 activation, achieving the smallest memory footprint.

768 D.2 ON-DEVICE COMPUTATION
769

770 We report on-device computation as the total FLOPs executed on a single device over the entire
771 training process until it reaches the target accuracy. Let the number of global rounds be R , the number
772 of local iterations (epochs/passes) per round be E , and let $\text{Cost}_{\text{local}}$ denote the computation for one
773 complete local epoch under a given method.

774 • **FL-LoRA:** Each local epoch performs the full RoBERTa + LoRA (forward & backward).
775 $\text{Computation}_{\text{device}} = \text{Cost}_{\text{FT}(\text{full backbone, LoRA})} \times R \times E$.

776 • **SFL-LoRA (U-shaped split learning):** Only the non-offloaded layers performs LoRA on
777 device (forward & backward).
778 $\text{Computation}_{\text{device}} = \text{Cost}_{\text{FT}(\text{partial backbone, LoRA})} \times R \times E$.

779 • **FwdLLM-LoRA (forward-only with perturbations):** The device performs only forward
780 propagation; each round uses K local perturbation forwards.
781 $\text{Computation}_{\text{device}} = \text{Cost}_{\text{Infer}(\text{full backbone})} \times R \times K$.

782 • **Fed MobiLLM:** The device performs a single forward propagation traversal of its local
783 data (no local replay).
784 $\text{Computation}_{\text{device}} = \text{Cost}_{\text{Infer}(\text{full backbone})}$.

785 D.3 ON-DEVICE COMMUNICATION
786

787 We report on-device communication as the total amount of data a single device exchanges with the
788 server over the entire training process until it reaches the target accuracy. Let the number of global
789 rounds be R , the number of local iterations (epochs/passes) per round be E .

790 • **FL-LoRA:** In standard FL, devices and server exchange trainable parameters in both
791 directions (upload/downlink) each global round:
792 $\text{Communication}_{\text{device}} = 2 \times R \times |\theta_{\text{LoRA}}|$,
793 where $|\theta_{\text{LoRA}}|$ is the size of the on-device LoRA trainable parameters.

794 • **SFL-LoRA (U-shaped split learning):** Beyond the round-wise parameter exchange, split
795 learning requires frequent exchange of intermediate activations and backward gradients
796 during local forward/backward:
797 $\text{Communication}_{\text{device}} = 2 \times R \times |\theta_{\text{LoRA}}| + R \times E \times \text{Comm}_{\text{act/grad-per epoch}}$,
798 where $\text{Comm}_{\text{act/grad-per epoch}}$ denotes the activation/gradient traffic for one local
799 forward+backward epoch.

800 • **FwdLLM-LoRA.** Similar to FL-LoRA, the standard communication rhythm for federated
801 learning:
802 $\text{Communication}_{\text{device}} = 2 \times R \times |\theta_{\text{LoRA}}|$.

803 • **Fed MobiLLM:** The device performs a single forward propagation traversal of its local
804 data and uploads only a small subset of layer-wise activations selected by the token selector;
805 there is no parameter round-trip or gradient return:
806 $\text{Communication}_{\text{device}} \approx \text{Comm}_{\text{selected-activations- single epoch}}$.

810 D.4 TRAINING TIME TO TARGET ACCURACY
811

812 We report the training time to target accuracy for each LLM federated FT framework. Let the number
813 of global rounds be R , and define: t_1 — per-round on-device runtime, t_2 — per-round device–server
814 parameter communication time, t_3 — per-round server aggregation time.

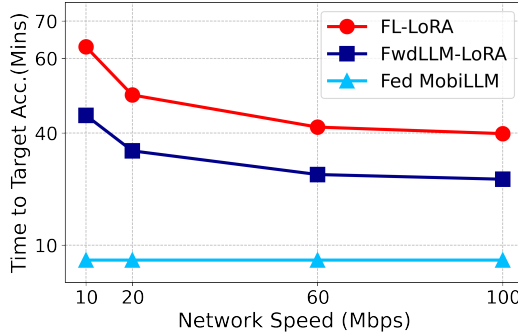
815 For **FL-LoRA / SFL-LoRA / FwdLLM-LoRA**, the per-round steps run *serially*, so
816

$$817 T_{\text{train}} = (t_1 + t_2 + t_3) \times R.$$

818 The only difference lies in t_1 :
819

- 820 • **FL-LoRA:** t_1 = on-device LoRA fine-tuning (forward + backward).
- 821 • **SFL-LoRA:** t_1 = split-learning based device–server co-training; frequent activation/
822 gradient exchange makes t_1 typically longer.
- 823 • **FwdLLM-LoRA:** t_1 = on device multiple forward propagations.

825 **Fed MobiLLM** does not follow a federated sequential rhythm. Instead, it overlaps single forward
826 propagation time on the device side with communication time and server iteration time in parallel.
827 The total training time approximates the maximum duration among these three components. In our
828 testing, the server iteration typically dominates, i.e., $T_{\text{train}} \approx t_{\text{server-iter}}$.
829

830 E DISCUSSIONS
831832 E.1 IMPACT OF NETWORK SPEED ON TRAINING EFFICIENCY
833

846 Figure 6: Impact of network speed on time-to-accuracy (homogeneous Xavier clusters, task:
847 RoBERTa-Base@MRPC).
848

849 In practical federated LLM fine-tuning, device–server communication makes training efficiency sensitive
850 to network conditions. Consequently, network fluctuations may impact overall training efficiency.
851 Figure 6 illustrates the training efficiency across methods under different wireless transmission speeds.
852 Since the total training time in FL-LoRA and FwdLLM-LoRA is affected by the communication
853 time, they suffer severe performance degradation under low-speed transmission conditions. For
854 example, FwdLLM-LoRA shows a 1.62 \times slowdown at 10Mbps vs. 100Mbps. In contrast, Fed
855 MobiLLM maintains stable total latency across different transmission speeds, demonstrating almost
856 no variations from 10 Mbps to 100 Mbps. Such resilience stems from parallel scheduling that
857 overlaps communication with device- and server-side computation, masking transmission delays with
858 on-device compute time that is unaffected by network-speed fluctuations.
859

860 E.2 SERVER STORAGE
861

862 As shown in Table 5, we report Fed MobiLLM’s server-side cache usage across different backbone
863 sizes (from RoBERTa-Base to OPT-1.3B) and dataset scales (from RTE to QNLI). When targeting
larger backbones or higher data throughput, edge servers with tight storage budgets may require

864

Table 5: Server cache size across backbones and tasks.

865

866

867

868

869

870

871

872

873

874

875

additional scalability measures for the caching mechanism. As future work, we will explore activation-aware quantization (e.g., mixed 2–4-bit precision per layer) and intelligent lifecycle management (automatically purging stale or low-impact activation–deviation samples) to align storage costs with operational budgets without compromising adaptation quality.

876

877

878

879

880

881

882

883

884

885

886

887

888

889

890

891

892

893

894

895

896

897

898

899

900

901

902

903

904

905

906

907

908

909

910

911

912

913

914

915

916

917